Int. J. Dev. Biol. 42: 385-392 (1998)

Segmentation of the vertebrate hindbrain: a time-lapse analysis

PAUL M. KULESA and SCOTT E. FRASER

Beckman Institute, California Institute of Technology, Pasadena, USA

ABSTRACT The chick hindbrain starts from a simple and relatively uniform axis and becomes segmented into repeating units, called rhombomeres. The rhombomeres become sites of cell differentiation into specific neurons and the location from which neural crest cells emerge from the neural tube to form the peripheral nervous system, which has only been analyzed at distinct time points due to the lack of a method to watch the neural tube as it is shaped into segments. We have developed a whole-embryo explant culture system in order to study cell and tissue movements with time-lapse video microscopy. Quantitative analyses of the neural tube during its segmentation show that not all rhombomeres are shaped by the same mechanism. In the rostral hindbrain, or first three segments, rhombomeres are shaped by an expansion in the lateral width of the mid-rhombomere; either a smaller expansion or a constriction takes place at the rhombomere boundaries. In the caudal hindbrain, the rhombomere boundaries constrict more than the mid-rhombomere lateral widths increase or decrease, leading to the shaping of the segments. Throughout the segmentation process the rostrocaudal lengths of all rhombomeres remain nearly constant indicating that shape changes are influenced by lateral expansions and constrictions of the neural tube.

KEY WORDS: *vertebrate, hindbrain, segmentation, whole-embryo explant, time-lapse*

Introduction

The process by which an organized structure arises from a homogeneous distribution of cells is a fundamental problem in Developmental Biology. García-Bellido pointed out that compartmentalized structures offer unique advantages and challenges for the study of patterning mechanisms (García-Bellido *et al.,* 1976). His experiments, and those of the countless number of researchers he has influenced, have exploited the compartmented and segmented structures in invertebrates and vertebrates (Stern and Ingham, 1992) to gain a better understanding of the processes by which regional specification takes place in the embryo.

During the assembly of the vertebrate nervous system, early cell interactions appear to establish a groundplan that guides the later development of the neural tube. In the hindbrain, the spatial groundplan is thought to be reflected in the physical shaping of the neural tube into 7 repeated segments, called rhombomeres (Vaage, 1969; Lumsden and Keynes, 1989). Each rhombomere has a distinguishable shape and is delineated by boundaries which form in a precise spatiotemporal order and not in a strict rostrocaudal sequence (Vaage, 1969). In dye labeling experiments, cells marked with a fluorescent dye intermingle extensively within a rhombomere and only a few cross a rhombomere boundary once it is formed (Fraser *et al.,* 1990; Birgbauer and Fraser, 1994), indicating that rhombomeres represent units of cell lineage restriction. Moreover, cell bodies of the cranial motor nerves in avian embryos form in pairs of rhombomeres (Keynes and Lumsden, 1990), providing further support for an underlying spatial plan. The segmented appearance of the hindbrain is transient, and eventually the shape of the neural tube returns to a less-obviously segmented cylinder.

Some molecular correlates of hindbrain morphogenesis in mouse and chick are known, as the expression domains of several genes have rostral, caudal or both limits that coincide with rhombomere boundaries. For example, members of the *Hox* gene family (Graham *et al.,* 1989; Wilkinson *et al.,* 1989) extend from caudal regions of the embryo to rostral limits at individual rhombomere boundaries. Other molecular patterns are spatially distributed within rhombomere restricted domains, such as Krox-20 mRNA and protein which are expressed in rhombomere 3 (r3) and r5 (Wilkinson, 1993). Many *Hox* gene transcripts (reviewed in Graham, 1992; Wilkinson, 1993) as well as intercellular signaling molecules in the EphA and EphB families (Nieto *et al.,* 1992) display both types of patterns. The timing of these gene expression patterns and the dynamic spatial

Abbreviations used in this paper: ss, somite stage; r, rhombomere; b, rhombomere boundary.

***Address for reprints**: Beckman Institute (139-74), California Institute of Technology, Pasadena, CA 91125, USA. FAX: 626-449-5163. e-mail: sefraser@druggist.gg.caltech.edu

0214-6282/97/$10.00

Printed in Spain

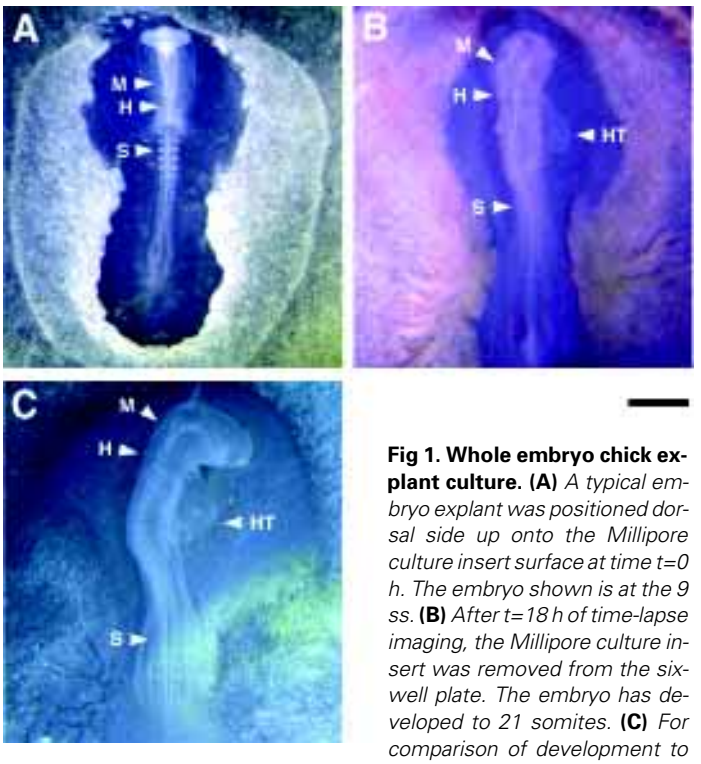

Fig 1. Whole embryo chick explant culture. (A) *A typical embryo explant was positioned dorsal side up onto the Millipore culture insert surface at time t=0 h. The embryo shown is at the 9 ss.* **(B)** *After t=18 h of time-lapse imaging, the Millipore culture insert was removed from the six-well plate. The embryo has developed to 21 somites.* **(C)** *For comparison of development to the explant cultures, we selected a 9 ss embryo and then reincubated the egg. After 18 h, the rotation of the intact embryo is nearly complete and the entire embryo appears larger in size than the embryo explant. The intact embryo has developed 21 somites. Some of the anatomical features are labeled, including the midbrain (M), hindbrain (H), heart (HT) and somites (S). Bar, 1 mm.*

variation offer the possibility that they are involved in the establishment or maintenance of the rhombomeric pattern (Krumlauf, 1993; Wilkinson, 1993,1995). Whether there is a spatiotemporal correlation between gene expression patterns and the appearance of rhombomere boundaries is not fully understood. Prior to the first morphological signs of segmentation, Krox-20 is expressed as a thin, horizontal stripe, which first appears in r3 and later in r5. The stripe expressions then widen to sharp boundaries which correspond with r3 and r5. Although no clear temporal patterns of gene expression have emerged which correlate to the spatial positions of the forming rhombomere boundaries, there is a tremendous need to develop a framework where molecular pattern data can be linked to the spatial and temporal events of the cell and tissue dynamics involved in the hindbrain shaping.

The primary cell and tissue mechanisms responsible for physically sculpting the hindbrain are still largely unknown. Boundary regions become distinct in the genes they express, the intermediate filaments they contain, and their extracellular environment (Heyman *et al.,* 1995), however, these aspects appear much later than the morphological shaping which initially defines the segments. Several mechanisms have been proposed for the morphogenesis of an individual rhombomere and the subsequent segmentation of the hindbrain (for a summary see Guthrie *et al.,* 1991). These range from rapid forward growth and localized expansion of the neural tube (Adelmann, 1925) to focal proliferation of cells coupled with a constraining structure at the boundaries causing a bulging out of the neural tube (Tuckett and Morriss-Kay, 1985). Studies of cell division in the chick hindbrain show that the density of mitotic cells is greater toward the centers of rhombomeres than in boundary regions (Guthrie *et al.,* 1991), suggesting that differences in cell proliferation might shape the rhombomeres. It remains unknown how such mitotic maxima are coordinated spatially and whether they are sufficient to sculpt the developing hindbrain. Thus, even basic questions, such as whether a rhombomere arises from an expansion of the neural tube or by a constriction at the rhombomere boundaries remain unanswered.

Here, we take advantage of the chick embryo to study hindbrain morphogenesis. The rapid segmentation process and the relatively simple geometry of the embryo growing in a 2-D horizontal plane permitted us to develop a whole-embryo explant culture method and perform time-lapse video imaging of hindbrain segmentation. To test the hypotheses of hindbrain segmentation, we observe and measure the physical shape changes of the neural tube during its segmentation into rhombomeres. The results suggest that no single mechanism or behavior accounts for hindbrain segmentation.

Results

Whole embryo explant cultures maintained normal morphology and growth rates for 1-2 days (Fig. 1). The growth of the embryo explants in culture was measured by counting the number

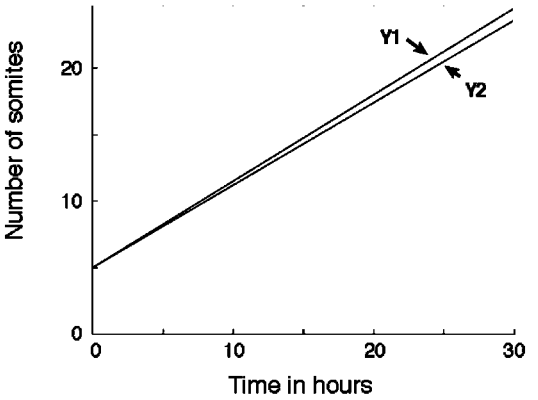

Fig 2. Comparison of growth rates for intact versus explant embryos. *The average growth rate for embryo explants was determined by counting the number of somites before and after each time-lapse session (n=24) as well as in several (n=36) embryos grown in explant culture and placed on the microscope stage within the thermal insulation unit surrounding the microscope. The average growth rate for intact embryos (n=60) was measured before and after a 10 h incubation period inside the thermally insulated microscope stage area used for time-lapsing. Since the number of somites in embryo explants grown in culture was counted at various times depending on the duration of the time-lapse, we assumed the growth rate was constant and calculated an average growth rate from the total number of embryo explants. We then constructed a line with slope equal to the average growth rate. For intact embryos, the average growth rate was also assumed to be constant throughout the 10-h incubation period and a line was constructed with slope equal to the average growth rate and extrapolated to t=30 h. The initial number of somites was arbitrarily chosen to be 5. The equations for the lines are: For explant embryos (Y1): y=ax + b; a=0.65 somites/h; b=5. For intact embryos (Y2): y=cx + d; c=0.62 somites/h; d=5.*

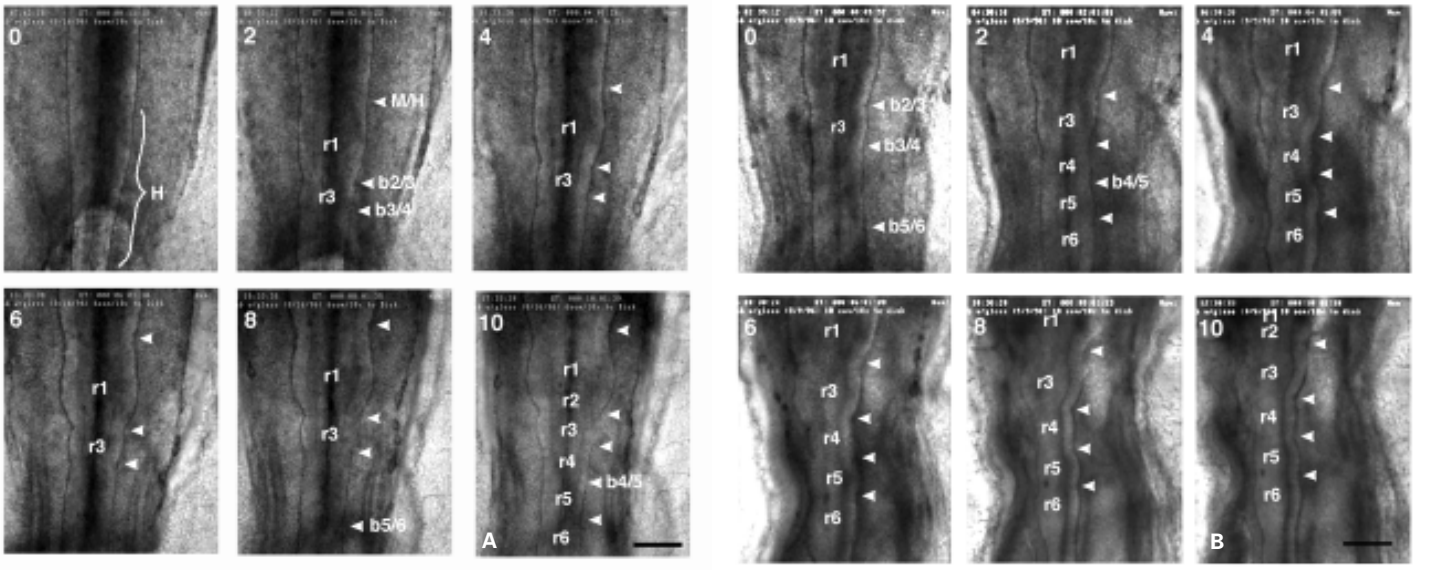

Fig. 3. Hindbrain segmentation sequence. *Each image is an individual brightfield image from a typical time-lapse sequence.* **(A)** *The first 10-h sequence from a typical time-lapse imaging session (n=12) of 6-8 ss embryos in two-hour increments: (0) the hindbrain region is labeled as (H); (2) morphological signs of the midbrain/hindbrain (M/H) boundary, b2/3 (the boundary between rhombomere 2 (r2) and r3), and b3/4 are visible. Rhombomere 1 and r3 are labeled; (8) b5/6 is visible; (10) b4/5 is visible.* **(B)** *The second 10-h sequence from a typical time-lapse imaging session (n=12) of 9-11 ss embryos in two-hour increments: (0) morphological signs of b2/3, b3/4 and b5/6 are visible; (2) b4/5 appears. Bar, 200 μm.*

of somite pairs before and after each time-lapse imaging session. For comparison to intact embryo growth, we staged, resealed and incubated a number of eggs in the same microscope incubator used for the time-lapse movies. After 10 h we assessed the growth by counting the number of somite pairs added. The average growth rate of embryo explants (n=60) was 0.65 somites/hour and of intact embryos (n=60) was 0.62 somites/hour (Fig. 2). In explant culture, the embryos did not flatten to the membrane; instead, they grew in 3-D suspension on a cushion of fluid between the membrane and the embryo (approximately 0.5 mm at the highest point). Although the embryo explants maintained their integrity and position on the membrane, they did not complete the rotation characteristic of a 22 somite stge (ss) embryo. After this stage, the embryo explant continued to add somites, but because of the failure to rotate, a 22 ss embryo explant somewhat resembled a 19 ss in ovo embryo. The youngest embryo explant was started at the 5 ss. Thus, the explant culture method appeared most useful for observing and analyzing dynamic events of chick development between the 5-19 ss.

We visualized the outline of the neural tube and the shaping of the hindbrain into segments in time-lapse video imaging sessions (n= 24). In explant cultures, the rhombomere boundaries appeared in the same spatial order as in intact embryos, however the time over which they formed was lengthened by 2-4 h. Figure 3A shows a time-series of still images from a typical embryo explant. Notice in Figure 3A, at t= 0 h the shape of the neural tube is a uniform tapered cylinder, with no discernible expanded or constricted regions (the rhombomere boundary between r5 and r6, b5/6, has formed by this time but is just caudal to the field of view). The first signs of b3/4 occurred 2 h later as the neural tube appeared to constrict inwards [Fig. 3A (2h), arrow]. At this time, b2/3 appeared as a small indentation of the neural tube and the midbrain/hindbrain boundary appeared to be forming as a broadly-rounded constriction [Fig. 3A (2h), arrow]. By t=6 h, the shapes of r1 and r3 became distinct as the mid-rhombomere areas have bulged outward. By 10 h, although the segmented shape of the rostral hindbrain was visible, the caudal regions of r4-r6 still appeared mostly unsegmented.

During the second 10-h (9-11 ss embryo explants) time lapse imaging sessions, the caudal portion of the hindbrain was noticeably shaped into segments (Fig. 3B). At t=0 h, the caudal hindbrain was still fairly unsegmented. By t=4 h the shapes of r4-r6 were more discernible. Between t=6 and t=10 h, the walls of the neural tube began to spread out laterally, leaving the appearance of a less segmented structure. This rapid lateral spreading of the neural tube occurred uniformly along the rostrocaudal axis, and not in any precise spatiotemporal order characteristic of the rhombomere formation sequence.

The average lateral widths of the neural tube, measured as the lateral distance between the pial walls (Fig. 4) are plotted at 1-h intervals providing a representation of how the widths of the neural tube varied in time (Fig. 5A,B,C). There was a large, steady increase in the lateral width at mid-r1. Surprisingly, the lateral width of b2/3 did not constrict, but increased gradually in a similar way to the expansion of mid-r3. The change in lateral width of b2/3 was nearly equal in magnitude to the change in width of mid-r3, which increased, but only about one-third as much as mid-r1. The lateral widths at b3/4 and mid-r4 both decreased, but in different ways during the time-lapse sessions. During the first 3 h, the lateral width at b3/4 was constant, but then decreased; its overall width change was slightly larger in magnitude than the mid-r3 expansion. The lateral width at mid-r4 increased during the first 3 h, but then decreased so that its change in width was the same amount as b3/4. Table 1 lists the average lateral widths of the neural tube at t=0 h and t=10 h of the time-lapse sessions as well as the overall change in the lateral widths.

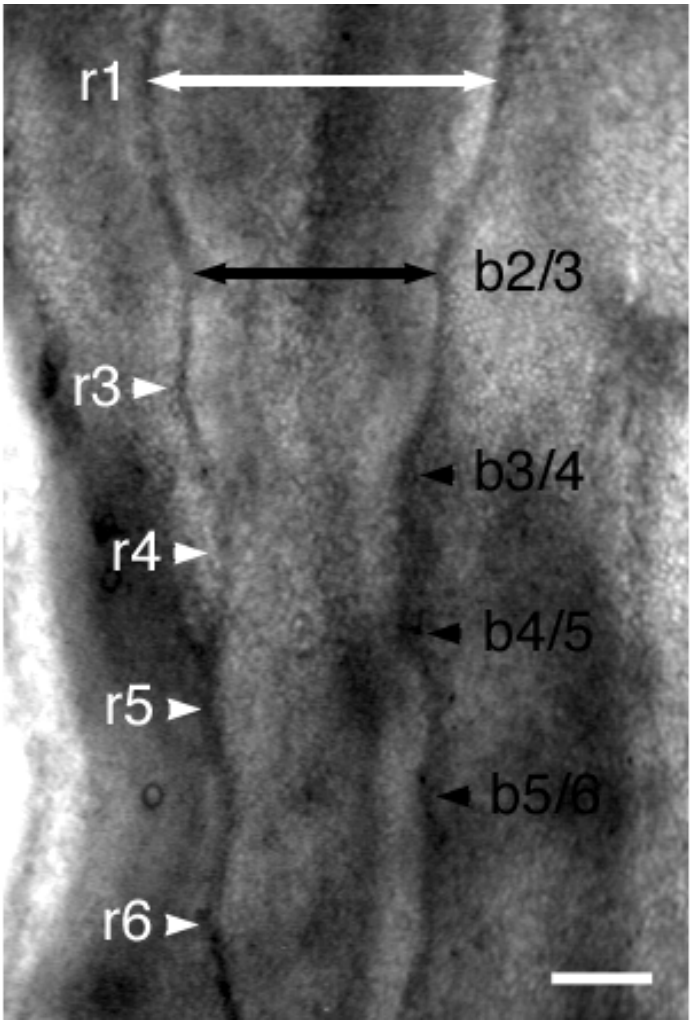

Fig. 4. Measurements. *The lateral width was measured at the 9 spatial locations shown: (i) the maximum lateral width (white) of r1, r3, r4, r5 and r6; (ii) the boundaries (black) b2/3, b3/4, b4/5, b5/6. Bar, 100 mm.*

We plotted the maximum lateral width of the neural tube at r1-r6 (Fig. 5B) and b2/3, b3/4, b4/5 and b5/6 (Fig. 5C). Notice in the figures that the average lateral width of mid-r1 expanded steadily throughout the 10-h periods (Fig. 5A,B). The lateral widths at the boundary b2/3 and mid-r3 increased at a similar rate and magnitude (Fig. 5A). The lateral widths at the boundaries b3/4, b4/5 and b5/6 all slightly decreased during the first 5 h, but then the lateral widths at b4/5 and b5/6 remained constant while the lateral width at b3/4 expanded back to nearly its width at t=0 h (Fig. 5C). The lateral widths of r4, r5 and r6 were initially nearly constant, then decreased slightly from 3-7 h before leveling off (Fig. 5B).

The lateral widths before and after the time-lapse sessions and the overall width changes are shown in Table 1. The average lateral width of mid-r1 increased in magnitude more than any other mid-rhombomere or boundary width. The lateral widths of mid-r3 and b2/3 expanded with nearly the same change in magnitude from their original widths. In the caudal hindbrain, or r4-r6, the lateral widths of the neural tube at the mid-rhombomeres and boundaries decreased, however the magnitude of the boundary

TABLE 1

LATERAL WIDTHS OF THE NEURAL TUBE BEFORE AND AFTER TIME-LAPSE IMAGING OF EMBRYO EXPLANTS

Lateral widths [6-8 ss (*n* = 12)]	W1 (±s.d.1) time = 0 h	W2 (±s.d.2) time = 10 h	Δ = W2 - W1	P
r1	226 (±27)	300 (±34)	74	< 0.001
r3	183 (±20)	204 (±26)	21	0.025
r4	170 (±21)	144 (±27)	-26	0.01
b2/3	183 (±19)	200 (±28)	17	0.05
b3/4	170 (±20)	144 (±21)	-26	0.005
[9-11 ss (*n*=12)]				
r1	261 (±20)	304 (±26)	43	< 0.001
r3	196 (±12)	230 (±21)	34	< 0.001
r4	174 (±12)	161 (±19)	-13	0.025
r5	178 (±16)	165 (±13)	-13	0.025
r6	174 (±15)	161 (±16)	-13	0.025
b2/3	187 (±18)	222 (±30)	35	0.005
b3/4	170 (±13)	165 (±24)	-5	0.25
b4/5	174 (±14)	148 (±16)	-26	< 0.001
b5/6	170 (±15)	148 (±12)	-22	< 0.001

W1 and W2 represent averaged (*n* = 12) values for each set of time-lapse imaging sessions. *P* values were calculated by the student's *t*-test. All measurements are in μm, except for the last column.

constrictions were nearly twice as large as the decrease in mid-rhombomere widths, leaving the appearance of segments in this region. In comparison to the first 10-h time-lapse sessions (6-8 ss embryo explants), the corresponding lateral widths of the neural tube in 9-11 ss embryo explants changed with nearly the same magnitude indicating that the rostral hindbrain or first 3 segments continued to be shaped in a similar manner. To determine whether there were any length changes in the rhombomeric segments of the explanted hindbrains during the segmentation

TABLE 2

ROSTROCAUDAL LENGTHS OF THE NEURAL TUBE IN EMBRYO EXPLANTS MEASURED BEFORE AND AFTER TIME-LAPSE IMAGING SESSIONS

Rostrocaudal lengths [6-8 ss (*n* = 12)]			L1 (±s.d.1) time = 0 h	L2 (±s.d.2) time = 10 h	Δ = L2 - L1	P
From	l	to				
mid-r1	l	b2/3	100 (±21)	104 (±17)	4	0.25
b2/3	l	b3/4 (r3)	113 (±4)	118 (±8)	5	0.05
b3/4	l	mid-r4	43 (±8)	52 (±8)	9	0.01
[9-11 ss (*n* = 12)]						
From	l	to				
mid-r1	l	b2/3	113 (±21)	96 (±13)	-17	0.025
b2/3	l	b3/4 (r3)	114 (±13)	106 (±8)	-8	0.05
b3/4	l	b3/4 (r4)	94 (±13)	90 (±8)	-4	0.25
b4/5	l	b5/6 (r5)	90 (±8)	94 (±4)	4	0.10
b5/6	l	mid-r6	57 (±13)	61 (±13)	4	0.25

L1 and L2 represent averaged (*n* = 12) values for each set of the time-lapse imaging sessions. *P* values were calculated using the student's *t*-test. All measurements are in μm, except for the last column.

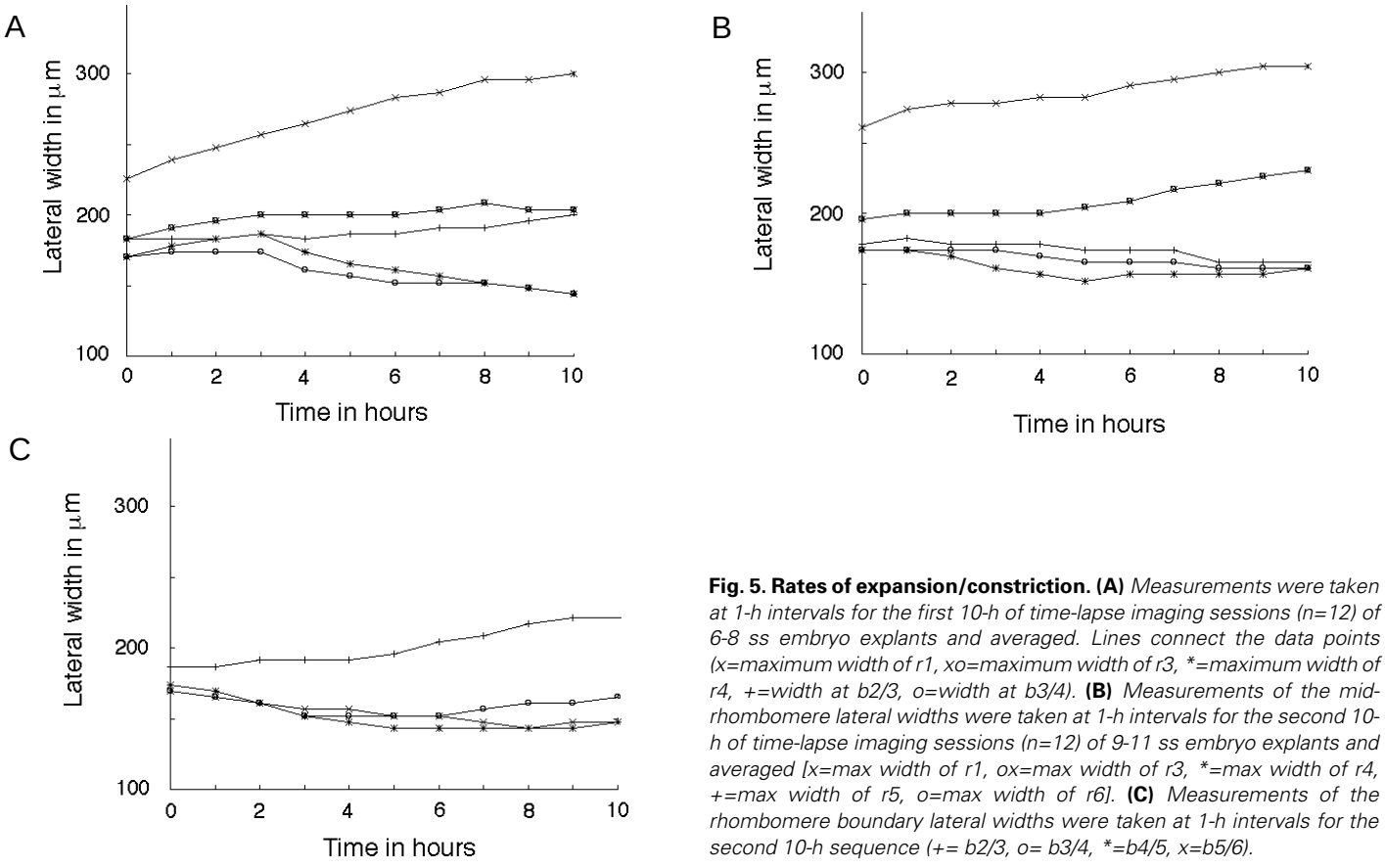

Fig. 5. Rates of expansion/constriction. (A) *Measurements were taken at 1-h intervals for the first 10-h of time-lapse imaging sessions (n=12) of 6-8 ss embryo explants and averaged. Lines connect the data points (x=maximum width of r1, xo=maximum width of r3, *=maximum width of r4, +=width at b2/3, o=width at b3/4).* **(B)** *Measurements of the mid-rhombomere lateral widths were taken at 1-h intervals for the second 10-h of time-lapse imaging sessions (n=12) of 9-11 ss embryo explants and averaged [x=max width of r1, ox=max width of r3, *=max width of r4, +=max width of r5, o=max width of r6].* **(C)** *Measurements of the rhombomere boundary lateral widths were taken at 1-h intervals for the second 10-h sequence (+= b2/3, o= b3/4, *=b4/5, x=b5/6).*

process, we measured the rostrocaudal distance between the mid-rhombomere and rhombomere boundaries before and after the time-lapse sessions. The measurements are reported as lengths between mid-rhombomere and rhombomere boundaries (Table 2). We had previously identified these axial locations for lateral width measurements and noted that throughout the time-lapse sessions the maximum lateral width of a rhombomere corresponded very closely to the mid-rhombomere axial level. We found that the average rostrocaudal length of each rhombomere stayed nearly constant throughout the time-lapse sequences. For example, during the first 10-h time-lapse sequences, the distance from mid-r1 to mid-r4 lengthened by only 19 μm, or +7% of its original length. In the second 10-h sequences, the distance from mid-r1 to mid-r6 actually shortened by 13 μm, or about -3% of its original length. Both r3 and r4 shortened, r3 by twice as much as r4, and r5 lengthened by the same amount that r4 shortened. The midbrain/hindbrain boundary and b6/7 were not often in the field of view for the entire time-lapse sessions which inhibited the measurements of the lengths of r1 and r6. We did notice a rostral shift of the entire hindbrain, which averaged about 13.5 μm/h. We attributed this movement to the addition of new somites, as time-lapse video recordings of somite growth implied that the caudal addition of structure drove a rostral progression of the entire embryo.

As a comparison to the hindbrain shape changes in explant culture, we measured the neural tube lateral widths of intact embryos at the same mid-rhombomere and rhombomere boundaries using two separate methods. In the first method we analyzed the same animal, measuring the neural tube lateral widths of 6-8 ss embryos, reincubating the eggs and re-measuring the lateral widths after 10 h. In the second method, we measured the neural tube widths of embryos taken from eggs at the 6-8 ss and 12-14 ss, with the assumption that the 12-14 ss embryos represented the expected stages to which 6-8 ss embryos would grow over a period of 10 h, based on our growth data. Table 3 presents the data for both methods. Notice in the table, that both comparison methods showed similar changes in the lateral widths of the rhombomere and rhombomere boundaries of intact embryos. That is, all of the neural tube lateral widths increased and by approximately similar magnitudes. The magnitude of the neural tube lateral widths appear smaller in Method 1, which may have been due to the difficulty in clearly identifying the precise lateral extent of the neural tube of *in ovo* embryos. In comparison to embryo explants, the lateral widths of the intact embryos at mid-r1, mid-r3 and b2/3 increased and with nearly the same magnitude as the changes seen in embryo explants (the change in mid-r3 was slightly larger in the intact embryo cases). In contrast, the lateral widths of intact embryos at mid-r4 and b3/4 increased by nearly the same magnitude that they decreased in the embryo explants.

Discussion

The last decade of hindbrain research has focused on identifying the molecular network underlying the segmentation process and whether this segmental structure guides the pattern of the emigrating neural crest cell population. With the exception of

TABLE 3

COMPARISON MEASUREMENTS OF LATERAL WIDTHS OF THE NEURAL TUBE IN INTACT EMBRYOS

Lateral widths (Method 2)	W1 (±s.d.1) time = 0 hrs	W2 (±s.d.2) time = 10 hrs	Δ = W2 - W1	P
r1	222 (±13)	300 (±17)	78	< 0.001
r3	178 (±9)	235 (±17)	57	< 0.001
r4	148 (±13)	183 (±22)	35	< 0.001
b2/3	178 (±9)	226 (±22)	48	< 0.001
b3/4	152 (±13)	178 (±22)	26	< 0.001
Lateral widths (Method 1)	W1 (±s.d.1) (6-8 ss embryos)	W2 (±s.d.2) (12-14 ss embryos)	Δ = W2 - W1	P
r1	130 (±11)	197 (±16)	67	< 0.001
r3	103 (±15)	148 (±19)	45	< 0.001
r4	85 (±10)	117 (±14)	31	< 0.001
b2/3	103 (±14)	130 (±12)	27	< 0.001
b3/4	85 (±10)	108 (±13)	22	< 0.001

Method 1 measured the lateral widths in the same animal and the table displays the averaged (n = 12) values at time = 0 hrs and time = 10 hrs. Method 2 measured the lateral widths in 6 - 8 ss embryos (n = 12) and in 12-14 ss embryos (n = 12) and the table displays the averaged values. P values were calculated by the student's t-test. All measurements are in μm, except for the last column.

studies of the patterns of cell division in the rhombomeres (Guthrie *et al.,* 1991) and the later development of rhombomere boundaries (Heyman *et al.,* 1995), there has been little focus on the cell and tissue dynamics which shape the hindbrain segments. Our study is meant to capture cell and tissue dynamics during the shaping of the chick hindbrain and in this way offer the spatial and temporal data needed to link the cellular dynamics with the underlying patterns of gene expression.

Previous models of hindbrain segmentation have emphasized a variety of potential mechanisms. Adelmann (1925) suggested focal cell proliferation expanded the neural tube walls within rhombomeres, while rostrocaudal growth of the hindbrain caused the neural tube to pinch in at weakened sites. In order to indirectly test whether focal cell proliferation creates the segments, we measured the lateral width of the neural tube at mid-rhombomere and rhombomere boundaries. Our results show that different rhombomeres are shaped by different processes, even in the same animal. In the larger rhombomeres, r1 and r3, the expansion of the neural tube walls at mid-rhombomere dominates. The rhombomere boundary, b3/4 appears by a constriction; however, b2/3 becomes apparent even as it is expanding. The expansion of b2/3 suggests that rhombomeres are not shaped merely by focal growth or by focal constriction; instead two separable processes, constriction and expansion, may be taking place. In the r4, r5 and r6 region, the rhombomere boundaries constrict more than the mid-rhombomere widths expand or decrease to shape the caudal segments, suggesting that there may be less focal proliferation in the mid-rhombomeres or a stronger constriction at the rhombomere boundaries. To test the hypothesis of rostrocaudal growth of the hindbrain, we measured the distances between mid-rhombomeres and rhombomere boundaries during the segmentation process. Our results show that the rostrocaudal lengths of the rhombomeres remain nearly constant throughout the segmentation process, contradicting this hypothesis. It seems that the constrictions do not occur due to a weakened wall but must appear by a different mechanism. Thus, our results suggest that no single, simple mechanism is responsible for creating the shape changes which define the rhombomeres.

The comparison of hindbrain shape data in intact embryos to embryo explant measurements showed common and contrasting features. In both embryo explants and intact embryos, the width of the neural tube increased at mid-r1 and mid-r3. The increase in lateral width of b2/3 in intact embryos supported our time-lapse measurements in embryo explants which showed that the pinching in of the boundary b2/3 appeared even though its lateral width steadily expanded. In contrast, the lateral widths of mid-r4 and b3/4 increased in intact embryos but decreased in embryo explants. We cannot explain this difference, but offer that it may be difficult to establish the accurate width changes of the hindbrain in intact embryos based on data pieced together data from measurements in the same animal or on a representation of embryos from various stages. The subtleties that we noticed in the shaping of the hindbrain in embryo explants pointed out that there was an interplay of expansions and constrictions of the neural tube which shaped an individual rhombomere. Some mid-rhombomere or boundary widths did not necessarily only expand or only constrict throughout the segmentation, but did both during the course of the time-lapse.

As a comparison, we can consider our results in relation to other species. In rat, the shape of a segment is proposed to be due to a longitudinal expansion of the neural tube which when constrained by boundary regions causes the outer wall of the neural tube to bulge outwards (Tuckett and Morriss-Kay, 1985). Their observations of arrangements of microfilaments along the ventricular wall of the neural tube and fan-shaped arrays of microtubules at the boundaries suggest the possibility of a special structural integrity of these areas. The longitudinal expansion of the neural tube is thought to be a result of oriented cell divisions. In chick, although there appears to be no preferred orientation of cell division in the hindbrain, a similar class of structures along the ventricular wall within rhombomeres (Guthrie *et al.,* 1991) and at the boundaries (Heyman *et al.,* 1995) have been reported in older (St. 17) embryos, which is too late to be involved in the initial shaping process. As of yet, no systematic approach in rat has been undertaken to capture the temporal cellular events which could reveal the physical aspects of segmentation, such as the formation of the constraining boundaries and the longitudinal expansion of the neural tube forcing the bulging of the neural tube wall.

Our studies are meant to be a first step toward a systematic approach in chick to analyze the cell and tissue dynamics of hindbrain segmentation. Our whole embryo explant culture method has allowed us to look at the dynamic tissue shaping events involved in the formation of each segment. The next steps will be to fluorescently label and follow hindbrain cells in order to observe the events which underlie the physical shaping process, permitting the synthesis of the local cell movements with the tissue dynamics. It is only when the cell and tissue level data are integrated together in a detailed model that we will know if we are drawing closer to an understanding of a mechanism for hindbrain segmentation.

Materials and Methods

Embryos

Fertile White Leghorn chick eggs were acquired from a local supplier (Lakeview Farms) and incubated at 38°C until approximately the 6-11 somite stage (ss) of development. Eggs were rinsed with 70% alcohol and 3 mL of albumin was removed prior to cutting a window through the shell. A solution of 10% India ink (Pelikan Fount; PLK 51822A143) in Howard Ringer's solution was injected below the blastodisc to visualize the embryos. Embryos were staged according to the stages of Hamburger and Hamilton (1951), denoted as St.10, for example; in other cases, the embryos were staged by their number of somites, denoted as 10 ss, for example.

Culture preparation

Embryos at the 6-8 ss and 9-11 ss were removed from the egg for explant culture by placing an oval ring of filter paper around the circumference of the embryo, cutting around the ring and then removing the ring with the embryo attached into Ringer's solution. The paper ring was approximately 1.5 cm along the major axis with a hole wide enough to provide ample space between the inner side of the ring and the embryo. This leaves the whole embryo intact and includes a portion of the surrounding blastoderm to a diameter equal to the outside diameter of the paper ring. The excised embryo was cleansed of yolk platelets and india ink by gently blowing Ringer's solution across it with a P-200 pipetman (Rainin). Explant cultures were created using Millicell culture inserts (Millipore #PICM 030-50) and six-well culture plates (Falcon 3046), similar to a previous protocol (Krull *et al.,* 1995). The Millicell insert surface was pre-coated with 200 μL of fibronectin (Sigma #F-2006, diluted 1:50 in phosphate buffer), and the excess pipetted away. The dorsal surface of the embryo was placed on the Millicell membrane, leaving the ventral surface exposed to the atmosphere. Excess Ringer's solution was pipetted off the membrane surface at the rostral and caudal ends of the explant so that the flow of the draining solution straightened the embryo's rostrocaudal axis. This naturally spread the explant without flattening the embryo and mimicked the tension of the blastoderm normally created by the stretching of the yolk sac. Each explant covered approximately two-thirds (~2.8 cm^2) of the membrane surface area of the Millicell insert. The insert was then placed in one well of the six-well plate. The Millicell insert was underlain with a defined culture medium composed of Neurobasal medium (Gibco #21103-031), supplemented with B27 (Gibco #17504-036) and 0.5 mM L-glutamine (Sigma #G-3126). Sterile water was added to the unfilled wells of the culture plate to minimize dehydration during the time-lapse sequences. The entire six well plate was then sealed along its sides with parafilm.

Time-lapse video microscopy

Hindbrain segmentation in culture explants was followed by low-light-level video microscopy (transmitted light). The six-well culture plate was placed on the stage of a Zeiss Axiovert microscope that was surrounded by an insulated box with two enclosed warming incubators (Lyon Electric Co. Inc.; #115-020) that maintained the explant cultures at 38°C for the duration of the time-lapse filming, with only mild temperature fluctuations. For better image resolution, we modified the six-well culture plate by making a hole in the bottom of one of the wells into which a 25 mm round glass coverslip was sealed using silicone grease. The membrane of the Millipore culture insert is 12.7 μm thick and becomes transparent when moist. Images were obtained through a 10X objective (Zeiss Plan-Neofluar, Numerical Aperture (NA)=0.30) and recorded with a Hamamatsu 2400 silicon intensified target (SIT) camera. Each image was processed with frame averaging (16 frames) using the VidIm software package (Belford, Stolberg and Fraser, unpublished). VidIm controlled the shutters (Uniblitz, model D122) and the recording of images every 2 minutes onto either a video optical memory disk recorder (OMDR; Panasonic 3038) or digitally to magneto-optical disk (Pinnacle). Images collected to the OMDR can conveniently be played back, allowing for adjustments to the specimen or microscope. Images which were digitally recorded were played back as a movie using the image processing and analysis program, NIH Image 1.60 (Rasband and Bright, 1995).

Time-lapse data analysis

The outline of the neural tube was clearly visible in the brightfield images using a 10X objective which gave a field of view (~1000 μm x 750 μm) large enough to see details of the outline of up to 6 rhombomeres. We visualized the complete neural tube segmentation process in two overlapping time-lapse sequences, starting with 6-8 ss embryos (n=12) and 9-11 ss embryos (n=12); each sequence contained 10-15 h of recorded time-lapse video imaging of hindbrain segmentation. Because there was a loss of contrast in the explant tissue after 12 h it was difficult to visualize the precise outline of the neural tube and rhombomere boundaries for longer time periods. In each time-lapse video image, the outline of the neural tube appeared in a 2-D horizontal plane representing a coronal section of the neural tube, so that the measured shape changes represented the lateral width dynamics of the neural tube. We measured the lateral width of the neural tube as the distance between the pial walls of the neural tube, at the axial level of mid-rhombomeres and rhombomere boundaries. During the first 10-h sequence of brightfield time-lapse imaging, we followed the maximum lateral width of the neural tube at r1, r3 and r4, and b2/3 and b3/4. During the second 10-h sequence of imaging we measured the lateral width of the neural tube at all the major rhombomere levels; r1-r6, b2/3, b3/4, b4/5 and b5/6. Because the morphological features of b1/2 and b6/7 are very subtle, their widths were not measured. Measurements were made from tracings on a clear transparency placed over the video monitor. The rostrocaudal axis of the neural tube and the axial level of each mid-rhombomere and rhombomere boundary was marked on the last image in the series (t=10 h). The shapes of the rhombomeres and the boundary regions were more discernible at this time point. Working backwards in time, we measured the neural tube lateral widths at 1-h intervals. Using the identifed mid-rhombomere and rhombomere boundary locations, we also measured the rostrocaudal distances between these axial levels at t=0 and t=10 h to note if there were any changes in the length of the hindbrain from its segmentation.

Intact embryo comparisons

We used 2 different methods of analyzing the hindbrain shapes of intact embryos in order to compare to our measurements of rhombomere shaping in embryo explants. The first method imaged the hindbrain of the embryo in the egg using a microscope outfitted to accomodate placing an egg under an objective, while the second method removed a number of embryos at various stages from the egg and imaged the hindbrain in the same way as the embryo explants. Thus, the 2 different methods for comparison combined the advantages of leaving the embryo in the egg and imaging the hindbrain shape of intact embryos with the same microscopy set-up used for embryo explants. In the first method (before and after analysis of the same embryo), eggs were windowed and staged. Embryos at the 6-8 ss (n=12) were selected and the eggs placed under an upright microscope (Zeiss Axiophot) outfitted with a 10X super long working distance (SLWD) objective NA 0.21. Using a fiber optic light source to illuminate the embryo, still images of the hindbrain were recorded onto a video optical memory disk recorder (OMDR; Panasonic 3038). After recording the image, each egg was resealed and placed in the same thermal insulation unit used for time-lapse imaging of embryo explants. After 10 h, the eggs were re-opened and the hindbrain was again imaged. The lateral widths of the neural tube were measured at these 2 time points in the same manner as used for the embryo explants. In the second method (analysis of different embryos), eggs were windowed and staged. Embryos at the 6-8 ss (n=12) and 12-14 ss (n=12) were removed from eggs and placed in explant cultures in the same method used for embryo explants. Embryos at the 12-14 ss were chosen to correspond to the expected growth in 10 h of a 6-8 ss embryo based on our growth data of intact embryos incubated within the thermally insulated microscope area. Instead of using culture inserts, embryos were pipetted directly into wells (one embryo per well) of a six-well culture plate and positioned. Brightfield images of the hindbrain region were recorded and

the lateral widths of the neural tube were measured with the same microscope, objective and clear transparency method used for the embryo explant measurements.

References

ADELMANN, H.B. (1925). The development of the neural folds and cranial ganglia of the rat. *J. Comp. Neurol. 39:* 19-171.

BIRGBAUER, E. and FRASER, S.E. (1994). Violation of cell lineage compartments in the chick hindbrain. *Development 120:* 1347-1356.

FRASER, S.E., KEYNES, R.J. and LUMSDEN, A. (1990). Segmentation in the chick embryo hindbrain is defined by cell lineage restriction. *Nature 334:* 431-435.

GARCÍA-BELLIDO, A., RIPOLL, P. and MORATA, G. (1976). Developmental compartmentalization in the dorsal mesothoracic disc of *Drosophila*. *Dev. Biol. 48:* 132-147.

GRAHAM, A. (1992). Patterning the rostrocaudal axis of the hindbrain. *Semin. Neurosci. 4:* 307-315.

GRAHAM, A., PAPALOPULU, N., and KRUMLAUF, R. (1989). The murine and *Drosophila* homeobox gene complexes have common features of organisation and expression. *Cell 57:* 367-378.

GUTHRIE, S., BUTCHER, M. and LUMSDEN, A. (1991). Patterns of cell division and interkinetic nuclear migration in the chick embryo hindbrain. *J. Neurobiol. 22:* 742-754.

HAMBURGER, V. and HAMILTON, H.L. (1951). A series of normal stages in the development of the chick embryo. *J. Morphol. 88:* 49-92.

HEYMAN, I., KENT, A. and LUMSDEN, A. (1995). Cell and matrix specialisations of rhombomere boundaries. *Dev. Dynamics 204:* 301-315.

KEYNES, R. and LUMSDEN, A. (1990). Segmentation and the origin of regional diversity in the vertebrate central nervous system. *Neuron 2:* 1-9.

KRULL, C.E., COLLAZO, A., FRASER, S.E. and BRONNER-FRASER, M. (1995). Segmental migration of trunk neural crest: time-lapse analysis reveals a role for PNA-binding molecules. *Development 121:* 3733-3743.

KRUMLAUF, R. (1993). Hox genes and pattern formation in the branchial region of the vertebrate head. *Trends Genet. 9:* 106-112.

LUMSDEN, A. and KEYNES, R. (1989). Segmental pattern of neuronal development in the chick hindbrain. *Nature 337:* 424-428.

NIETO, M.A., GILARDI-HEBENSTREIT, P., CHARNAY, P. and WILKINSON, D.G. (1992). A receptor protein tyrosine kinase implicated in the segmental patterning of the hindbrain and mesoderm. *Development 116:* 1137-1150.

RASBAND, W.S. and BRIGHT, D.S. (1995). NIH Image: A public domain image processing program for the Macintosh. *Micro. Anal. Soc. J. 4:* 137-149.

STERN, C.D. and INGHAM, P.W. (1992). Papers presented at a meeting of the British Society for Developmental Biology at the University of Sussex. *Development (Suppl. U1.)*: N/A.

TUCKETT, F. and MORRISS-KAY, G. (1985). The ontogenesis of cranial neuromeres in the rat embryo II. A transmission electron microscope study. *J. Embryol. Exp. Morphol. 88:* 231-247.

VAAGE, S. (1969). The segmentation of the primitive neural tube in chick embryos (Gallus domesticus). A morphological, histochemical and autoradiographic investigation. *Ergeb. Anat. Entw. 41:* 3-87.

WILKINSON, D.G. (1993). Molecular mechanisms of segmental patterning in the vertebrate hindbrain and neural crest. *BioEssays 15 (8):* 499-505.

WILKINSON, D.G. (1995). Genetic control of segmentation in the vertebrate hindbrain. *Perspect. Dev. Neurobiol. 3(1):* 29-38.

WILKINSON, D.G., BHATT, S., COOK, M., BONCINELLI, E. and KRUMLAUF, R. (1989). Segmental expression of Hox-2 homeobox-containing genes in the developing mouse hindbrain. *Nature 341:* 405-409.